SURVEY OF TIGER MAIN ROTOR LOADS FROM DESIGN TO FLIGHT TEST

Kurt Götzfried
Eurocopter Deutschland GmbH
Ottobrunn, Germany

Abstract

The TIGER helicopter, developed as a joint venture between France and Germany, has been successfully flight-tested since April 1991. Five prototypes have chalked up more than 1700 flight hours. The TIGER main rotor is a powerful soft-inplane hingeless rotor for high controllability and agility with radial and conical elastomeric bearings (FEL concept).
Starting with a brief description of theoretical prediction methods, this paper addresses the whole process of load determination: predictions, critical evaluation of flight test results, measures for load reductions. Although the aircraft showed the expected flight properties from the start of testing, load optimisation was necessary to achieve a longer service life of critical main rotor parts and to expand the flight envelope. This process is structured as follows:
- Start of flight tests in April 1991. Reduction of 3/rev hub loads and tuning for low 4/rev vibrations.
- Hub geometry change from a 2.5° blade droop angle to a central 2.5° precone angle to expand the load factor capability by lowering loads in lead-lag bending and the control system. The structural set-up of the blade collar area was simultaneously reinforced and simplified.
- Shift of the 2nd lead-lag mode from 5.5/rev to 6/rev to reduce 4/rev torque amplitudes.
- Finally, a comprehensive stress flight campaign was performed for load cycle counting (approx. 30 flight hours, approx. 1000 single flight states), where the aircraft showed its structural fitness for mission task elements according to the tailored ADS 33C.
The general design goal of 6000 hours lifetime for all main rotor and control system parts (elastomeric bearings: 2500 hours) was achieved.

Notation

Ω	rotor speed
ΔMz	alternating lead-lag bending moment
μTAS	VTAS/$\Omega \bullet R$ advance ratio, based on true airspeed
A_b	$4 \bullet R \bullet c$; blade area
A/C	aircraft
ADS 33C	Army Aeronautical Design Standard
AFCS	Automatic Flight Control System
c	blade chord
C.G.	centre of gravity
CT/σ	$nz \bullet m \bullet g/\rho \bullet A_b \bullet (\Omega \bullet R)^2$
DLR	Deutsche Forschungsanstalt für Luft- und Raumfahrt
FAR	Federal Aviation Regulations
HAC	Hélicoptère anti Char
HAP	Hélicoptère d'appui et protection
kias	knots indicated airspeed
m	helicopter mass
MBB	Messerschmitt-Bölkow-Blohm
MCP	max. continuous power
MIL-S-8698	Military Specification
MMS	mast-mounted sight
MRSHAT01	main rotor shaft torque
Mß	flap bending moment
Mz	lead-lag bending moment
nz	load factor
ONERA	Office National d'Études et *Recherches Aéronautiques*
PAH2	Panzerabwehrhubschrauber, 2nd Gen.
Pst, PLL	rotating pitch link load
R	rotor radius
SLS	sea-level standard
$ß_0$	static flapping angle (elastic coning)
$ß_D$	built-in droop angle, rotor blade (preflap angle)
$ß_{elast.}$	elastic flapping angle
$ß_K$	built-in precone angle, rotor hub
$ß_P$	flapping angle velocity
TOW	take-off weight
VC	calibrated airspeed
VDIVE	maximum design speed
VH	max. horiz. speed, MCP
VIAS	indicated airspeed
VNE	never exceed speed

Introduction

When high controllability and manoeuvrability are required for a combat helicopter like TIGER, Fig. 1a, a hingeless main rotor system is an appropriate choice. Due to its relative high flap hinge offset (TIGER: 10%), a stiff main rotor system is able to transfer large control moments from the rotor to the fuselage, which significantly improves agility about A/C axes. However, the higher load situation compared, for instance, to articulated rotor systems (typical: 3%-5% hinge offset) requires greater structural strength of critical rotor parts. Before the adoption of fibreglass and composite materials, it was not possible to design rigid rotor systems which could stand the high structural loads by endowing their components with a long service life. One of the first successful designs with a rigid main rotor system was the BO105. The TIGER features a further improvement of the hingeless main rotor system: The FEL concept offers a simple design with few rotor parts. The use of elastomeric bearings allows both the replacement of the hitherto metal pitch bearings as well as the retention of the centrifugal force without tie bars.
This paper presents the successful load-optimisation process for the TIGER main rotor system, where it was possible to combine requirements for high agility and controllability with capabilities for taxiing and slope landings, which may generate critical loading conditions on rigid rotor systems.

1. The TIGER Main Rotor System

Before starting with a detailed look at the load behaviour of the TIGER main rotor, a short description of the system itself is given.
As already indicated, the TIGER main rotor is a further development of the rigid hingeless main rotor system (System BÖLKOW), which was realised for the first time on the BO105. The new design for the TIGER is called FEL, which stands for Fibre Elastomeric Bearing, /1/, see Fig. 1b. Its main characteristics are elastomeric bearings and composite materials for both the blades and the hub. In comparison to the BO105 main rotor, the FEL rotor offers an even simpler design with fewer parts, minimised maintenance and reduced vulnerability. The elastomeric bearings accomplish the blade pitch change, the transmission of the blade control moments into the hub and the support of the centrifugal force (conical elastomeric bearing).
A strong improvement in flight performance could be achieved thanks to the aerodynamic layout of the rotor blade: the new airfoils DMH3/DMH4, a joint development by the former MBB company and the German DLR, feature reduced drag at low and medium Mach numbers due to a wider laminar flow range compared to e. g. older profiles of the NACA series such as 0012, 23012. Suitability for high speeds is achieved through a high drag divergence Mach number, reduced compressibility effects on the advancing side of the rotor blade through a low outboard airfoil thickness of 9%, and the parabolic anhedral blade tip (changeable), designed by the French ONERA. The enhanced rotor solidity of 0.1 provides a low blade loading for 1g flight conditions and offers a growth potential for higher TOWs than the design mass of 5.4 metric tons. The blade frequency tuning has been optimised for low vibration by separating fundamental frequencies in flap/lag/torsion from rotor harmonics, Fig. 2.1a. The use of viscous fluid dampers ensures sufficient lead-lag damping for ground and air resonance stability. Excellent agility is provided by high control power (10% equivalent flap hinge offset supplies 5000 [Nm] control moment capacity per degree cyclic).
The technology applied serves to meet the handling qualities requirements of the tailored ADS 33C for aggressive manoeuvring.
Some main rotor characteristics are listed below:

TIGER Main Rotor Characteristics

rotor radius	6.5 [m]
blade number	4
blade chord	0.52 [m], airfoil part
profiles	DMH4, 12%, inboard DMH3, 9%, outboard
solidity	0.097 (thrust-weighted)
Lock number	10.16 at SLS
rotor speed, nom.	$\Omega = 34.46$ [1/s]
1st flap freq.	$\omega\beta/\Omega = 1.083$
1st lag freq.	$\omega\zeta/\Omega = 0.657$
1st torsion freq.	$\omega\Theta/\Omega = 4.76$, infinite grip
twist	12°, ref.: total radius
precone	2.5°
pitch axis offset	-0.01 [m], forward

2. Main Rotor Load Predictions and Calculation Techniques Applied

Estimating rotor loads is in general a complex task which requires a certain experience and high accuracy in the theoretical modelling of the rotor under development, see /2/, /4/, /7/. The actual process of rotor-load determination is iterative: predictions, checks through whirl tower and flight test results, refined rotor modelisations, measures for loads reductions, new flight tests... until the design goal is reached.

At EUROCOPTER Germany, different rotor codes are available for the aeromechanical modelisation of rotors as well as for the prediction of loads.
The following subchapters briefly describe the most important computer programs used for the TIGER main rotor sizing with reference to their load-relevant application:

2.1 Determination of Blade Eigenfrequencies and Blade Mode Shapes

The elementary tool for determining mode shapes and eigenfrequencies of a rotor blade is the computer program MOSES (mode shape estimation source), see Fig. 2.1a.
The code is based on a transfer matrix method, Fig.2.1b, extended to consider the influence of a centrifugal force field. The rotor blade is divided into segments and its structure is modelled by massless beam elements having only stiffness and inertia properties and discrete masses. Experience and special know-how are needed to introduce boundary conditions into this method for the hub attachment, spring elements or special rotor parts, e. g. elastomeric bearings.
Additional results of MOSES are the equivalent rigid body blade descriptions in flap/lag/torsion which are used in the STAN, BWVL codes. Another output is the radial distribution of a rotor blade's physical properties (mass, stiffness, inertia) as is needed for the input in aeroelastic rotor codes such as CAMRAD, C60.
The modelisation of the TIGER hub attachment is shown in Fig. 2.1c. The principle of an equivalent rigid body blade system is shown in Fig. 2.1d.

2.2 Trim and Steady Flight State Calculations

The stability and analysis code STAN is used for trim and steady flight state calculations (hover, horizontal flight domain, steady turns) with respect to dynamic flight analyses and/or rotor-load predictions.
It consists of a modelisation of the total aircraft including main and tail rotor, the fuselage, and stabilising surfaces, as well as of a more detailed model of the main rotor itself. The main rotor is primarily represented by equivalent rigid body blade systems, including the first modes of flap/ lead-lag/ blade torsion bending and the control system flexibility, Fig. 2.2a (fully coupled calculation). The blade itself is idealised versus radius by the distribution of mass, inertia, twist, chord, etc.. The aerodynamic part of the rotor model is based on the blade element theory, which applies two-dimensional airfoil data with corrections due to stall and compressibility. Three inflow models are available: a global (constant flow in the rotor disk), a local inflow model (constant flow in rotor disk segments) with trapezoidal distribution according to Prandtl/Glauert in forward flight, and a non-uniform inflow model developed by Pitt-Peters. The aerodynamic forces and the dynamic response of the rotor blades are calculated versus azimuth by a step-by-step integration of the differential equations of motion (Runge-Kutta).
Fig. 2.2b shows a comparison of test results/STAN calculation for the TIGER non-upgraded main rotor (DROOP version). The correlation is satisfactory regarding the dominating 1/rev content of the different blade load channels. The program results deteriorate, however, for high-stalled conditions with a significant higher harmonic content.

2.3 Blade Loads versus Radius

Blade loads versus radius are determined using the aeroelastic rotor codes CAMRAD and C60 (isolated rotor).
Only C60 is described here, because it was mainly used for TIGER load predictions:
The program was developed at the end of the Sixties by the BOEING VERTOL company, /4/. The model is based on a transfer matrix method similar to the "MOSES" code considering 10 harmonics (essential for the incorporation of higher harmonic excitation loads and blade bending modes). It features a fully developed, unsteady aerodynamic model (stall, compressibility, three-dimensional flow) including a non-uniform inflow model (prescribed wake).
Input data are the physical properties (from e. g. MOSES) and the airfoil characteristics of the rotor blade, trim data (from e. g. STAN) and a set of program control parameters. On the basis of accurate rotor modelling, C60 supplies suitable results for blade loads versus radius as well as pitch link loads for steady flight states up to the stalled region. In the case of the TIGER main rotor, predictions were carried out for the maximum blade loads vs. radius on the outboard portion of the blade, respectively pitch link loads along the theoretical CT/σ-stall curve for the non-upgraded main rotor (DROOP version).
A correlation of stress flight results with a C60 computation for the upgraded main rotor (PRECONE) is given in Fig. 2.3 for a 3g spiral turn load case for the blade torsion and lead-lag bending moment versus radius.

2.4 Manoeuvre Loads

A time domain simulation model (BWVL) is applied to calculate transient manoeuvre loads as required for strength certification according to FAR §29, Subpart C - Strength Requirements, and MIL-S-8698.
Typical manoeuvres are:

- symmetrical pull-ups
- negative g manoeuvres
- rolling pull-outs
- yaw manoeuvres
- spiral turns
- fast (180°) turns at constant height, e. g. 100ft
- roll reversals at load factors below and above 1g
- gust loads.

These so-called *static limit flight loads* have to be calculated at the structural load factor/speed boundary, applying maximum control input speeds. They represent safe loads and have to be multiplied by a safety factor of 1.5 for the static structural substantiation of all associated aircraft parts.
The physical modelisation of BWVL is similar to the STAN code, see above. Starting from trimmed conditions according to the input of disturbing control ramps or gusts, the time histories of the transient dynamic reactions of rotor and aircraft are calculated by a quasisteady step-by-step Runge-Kutta integration.
Fig. 2.4 shows a comparison between BWVL predictions and flight test results for the thrust/shaft bending moment envelope. The main reason for increasing the original limit was the expansion of the flight envelope.

3. Evaluation of Flight Test Results and Design Changes

Flight testing of the TIGER started in April 1991. The helicopter showed the expected controllability and thrust potential from the very beginning. However, an optimisation loop for loads and vibrations was necessary to enhance the service life of essential rotor parts and to expand the flight envelope. These steps towards systematic improvement are explained below.

3.1 Enhancement of the Shaft Bending Moment Limit

The first design estimation of the mast bending moment envelope was not appropriate. The estimated limit loads in shaft bending were reached during mission task elements flown in an aggressive manner, taxiing against strong wind (requirement: 50 [kts]) or slope landings. A boundary of 50,000 [Nm] was found to be adequate even for extremely aggressive mission task elements. The original and new shaft bending moment envelopes are given in Fig. 2.4.

3.2 Reduction of 3/rev Hub Loads and Tuning for low 4/rev Vibrations

3/rev vibrations resulting from the 2nd flap mode were unacceptably high in the transition speed range from 20 to 40 [kts] and at high speeds. The tuning capacity of the anti-vibration system SARIB, Fig. 3.2a, was exceeded. The solution was the adjustment of the 2nd flap mode well below 3/rev by some masses at halfspan of the rotor blade in combination with an adaptation of the flapper masses of the SARIB, /8/. Fig.3.2b indicates the achieved result to keep the 4/rev z-vibration level at both cabin stations of pilot and gunner below 0.1g up to a velocity of 250 [km/h] (max. level speed required for the PAH2).

3.3 Reduction of 4/rev Torque Amplitudes

The 4/rev torque amplitudes were found to be too high with respect to the service life of the flexible SARIB membrane, which is responsible for the transmission of the main rotor torque, see Fig. 3.2a. The reason was the close vicinity of the 2nd drive train mode (ca. 24 Hz) to the 4/rev (ca. 22 Hz, 104% RPM). An analytical study revealed that a shift of the 2nd lead-lag bending mode from 5.5/rev to 6/rev by trailing edge stiffening would lift the 2nd drive train mode by ca. 2 Hz, which offered an attenuation of nearly 50%. This theoretical prediction could be proven perfectly in the flight test, see Fig. 3.3.

3.4 Hub Geometry Change to Expand the Load Factor Capability

Flight test evaluations on the first prototype PT1 with respect to loads and lead-lag damping led to a trade-off study between the two aspects.
The initial main rotor design had a 2.5° preflap angle at the blade attachment (DROOP rotor), no precone angle, Fig. 3.4a. The design goal was to introduce more stabilising aerodynamic coupling - pitch up, flap up, lag back, called *negative pitch-lead-lag coupling*, see /3/, /5/. This was clearly

reached with the non-upgraded main rotor. The evaluation of ground and air resonance tests revealed comfortable stability margins.
On the other hand, as already indicated in STAN and C60 calculations versus load factor, the load behaviour was unsatisfactory, especially in high g-turns. A disadvantage of the so-called preflap coning is that the rotor blade has a greater distance to the pitch control axis compared to a preconed blade. Fig. 3.4a illustrates this kinematics effect. With reference to the same cyclic control input, this leads to higher 1/rev lead-lag bending moments, especially if the blade has a high elastic coning in the case of high g-turns. In consequence, higher 1/rev pitch link loads are provoked - the difference (flap bending - lead-lag bending) is an essential blade torsion contribution, see Fig. 3.4b. We recognise further that tailoring the stiffness of both flap and lead-lag in direction "matched rotor", where the stiffnesses are equal, offers an additional potential for the reduction of pitch link loads, /6/. But this has to be done very carefully because of a possible deterioration of the stable aeromechanical coupling behaviour, see above. The 1st pitch link harmonic itself is seen in the fixed control system as a zeroth harmonic, mainly in the swashplate tilting moment. Fulfilment of the requirement to have hydraulic control actuation up to at least 2.5g (5.4 [t], 120 [kts], SLS) in case of a single hydraulic failure was endangered. The static load capability on the forward control booster would probably have been reached at considerably lower g's, Fig. 3.4c.
The past load situation can be summarised:

- high loads in lead-lag bending:
  service lifetime of rotor blade, pitch links and elastomeric bearings endangered
- excessive loads on the forward control booster in case of a single hydraulic failure.

As too low lead-lag damping could be excluded due to the available viscous fluid dampers, in 1993 a hub geometry change was decided upon as a reasonable compromise between dynamic and load aspects. The 2.5° preflap angle was replaced by a 2.5° precone angle together with a reinforcement of the hub plates and the blade neck area. In flight tests this new "upgraded" main rotor demonstrated the achievement of the envisaged design goals:

- lower loads on blade, bearings, rotor head and control system resulting in a longer service life, see Fig.3.4c
- at the same time, the structure and the manufacturing process for the blade collar area could be simplified
- the load factor capability could be extended to the theoretical stall boundary of the new profiles, see Fig. 4.5.

4. Stress Flight Campaign and Demonstrated Flight Envelope

The load-determination process was rounded off by a comprehensive stress flight campaign performed for load cycle statistics (rain flow cycle counting). In 30 flight hours, approximately 1000 single flight states were flown on two prototypes PT1 (PAH2/HAC) and PT2 (HAP), see TIGER flight spectrum, Table 4. Thirty main rotor and control system load channels were instrumented for on-line monitoring during the flight tests and for data acquisition.
The aircraft demonstrated its total fitness for all relevant combat mission task elements in a wide flight envelope. Parameters were greatly varied: e. g. helicopter mass and centre of gravity, Fig. 4.1; load factor and speed, see comparison with structural design envelope, Fig. 4.2; rotor speed range in autorotation, Fig. 4.3; speed versus altitude, see fixing of VNE-boundaries, Fig. 4.4. The tests included flights with AFCS ON/OFF, wind speeds up to 50 [kts], sideslip angles up to 20° at maximum horizontal speed, and lateral flights up to 50 [kts] left/right.
Blade loadings CT/σ were even found to be above the theoretical stall curve (better: controllability limit) for the new DMH4/DMH3 profiles, see Fig. 4.5. Here it has to be admitted that the stub wing which serves as the weapon carrier may deliver some contribution, which has been estimated to be at best 5% of CT/σmax.
In Fig. 4.6, the shaft bending moment as a function of the lead-lag bending moment is presented as determined during the flight-stress measurements. A trend seems to be interesting towards the division of flight states into flap intensive ones (aggressive mission task elements, slope landings, taxiing) with low drag loads and lead-lag intensive ones (pull-ups, rolling pull-outs, spiral turns) with moderate flapping loads. In the case of slope landings, taxiing lead-lag bending is only provoked by Coriolis forces. High drag loads in the second group are provoked by high elastic blade coning ($\Delta Mz \sim \beta_0 \bullet \beta_p$), high speed, stall effects and high cyclic control input, whereas the relative small C.G. range of the TIGER, Fig. 4.1, limits the necessary shaft bending trim moments.
During the stress flight campaign, no severe structural overstressing problems were encountered. Good manoeuvrability was possible even at the extremes of the flight envelope without excessive vibrations.
The design goal of 6000 [hrs] lifetime for all main rotor and control system parts (elastomeric bearings: 2500 [hrs]) was achieved with respect to the specified TIGER flight spectrum (Table 4).

5. Conclusion

A brief description of the load-development process for the TIGER main rotor has been presented. Though the original rotor already showed the expected excellent flight-mechanical and aerodynamic behaviour during the first flight tests, optimisation was necessary to enhance the service life of critical main rotor parts as well as to expand the flight envelope. The aeromechanics computer programs used have proven to be reliable with respect to predictions and correlations. Nevertheless a strong feedback from flight tests is necessary because an overall load survey has to be understood as an iterative process of calculation and testing. In addition, the sizing of a rotor is an interdisciplinary task which has to combine different aspects from dynamics, flight mechanics, aerodynamics and strength to fulfil the design goals of a specified flight envelope. The development of the TIGER FEL main rotor was a challenge for all the engineers involved. It has now revealed its excellent performance for operational use.

Acknowledgements

The author would like to thank his colleagues M. Chapuis, A. Kellerer, G. Seitz, F. Dax, M. Doctorczyk, W. Popp, C. Kampa, H. Strehlow, D. Braun, W. Sinn and R. Wennekers for their contributions of material and advice. The author also wishes to express his thanks to the flight test centre in Marignane for good co-operation during the stress flight campaign.

References

1. D. Braun, H. Frommlet, A. Schwarz
"FEL - A NEW MAIN ROTOR SYSTEM"
Messerschmitt-Bölkow-Blohm GmbH
12th European Rotorcraft Forum
Garmisch-Partenkirchen, Germany, Sept. 1986

2. G. Reichert
"Loads Prediction Methods for Hingeless Rotor Helicopters"
Messerschmitt-Bölkow-Blohm GmbH
AGARD Conference Proceedings No. 122
Milan, Italy, March 1973

3. H. Huber
"Helicopter Aerodynamics and Dynamics"
Messerschmitt-Bölkow-Blohm GmbH
AGARD Lecture Series No. 63

4. R. Gabel
"Current Loads Technology for Helicopter Rotors"
Boeing Vertol Company, Vertol Division
AGARD Conference Proceedings No. 122
Milan, Italy, March 1973

5. K. H. Hohenemser
"Hingeless Rotorcraft Flight Dynamics"
Washington University, St. Louis, Missouri, USA
AGARDograph No. 197
September 1974

6. R. E. Hansford, I. A. Simons
"Torsion-Flap-Lag Coupling on Helicopter Rotor Blades"
Westland Helicopters, Yeovil, Somerset, England
Journal of the AHS, October 1973

7. B. Masure et A. Vuillet
"Méthodes de Calcul des Charges sur Rotor utilisées à l'Aérospatiale et Recoupements Expérimentaux"
Aérospatiale, Marignane, France

8. G: Seitz, T. Krysinki
"Overview of TIGER Dynamics Validation Program"
EUROCOPTER DEUTSCHLAND/FRANCE
48th AHS Forum, Washington, June 1992

9. R. Wennekers
"Loads, Dynamics/Vibrations, Acoustics"
EUROCOPTER 81663 München, Germany
AGARD LECTURE SERIES 209, May 1997

10. R. Wennekers
"Helicopter Weapon System Integration - Session 4: Case Histories: TIGER"
EUROCOPTER 81663 München, Germany
AGARD LECTURE SERIES 209, May 1997

11. K. R. Spreuer
"Results of the AH-64 Structural Demonstration"
Hughes Helicopter Inc., Carlsbad, California
38th Annual Forum of AHS, May 1982

12. F. S. Tse, I. E. Morse, R. T. Hinkle
"Mechanical Vibrations - Theory and Applications", 2nd edition
CBS Publishers & Distributors, Delhi, India

Fig. 1a: Test vehicle TIGER PT1 in PAH2 configuration

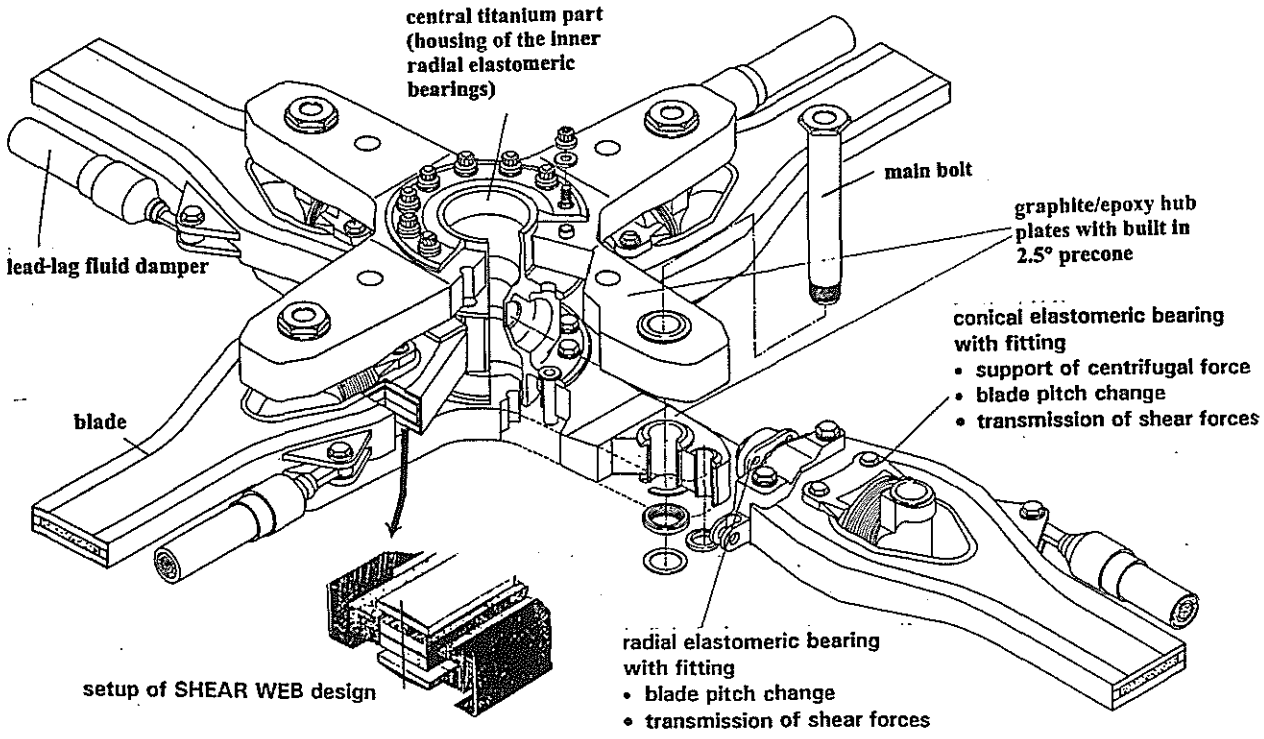

Fig. 1b: The TIGER hingeless main rotor concept (FEL)

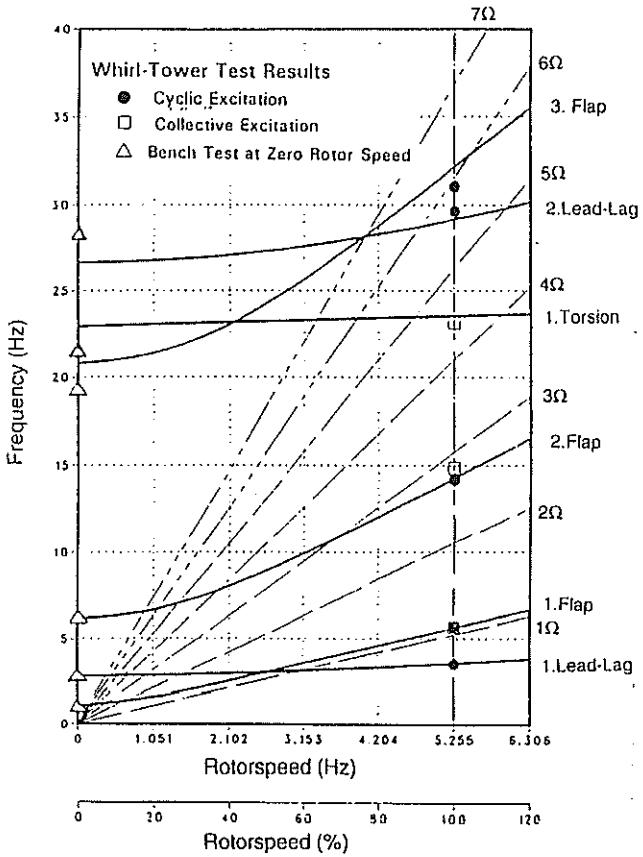

Fig. 2.1a: Eigenfrequency-Diagram, TIGER MAIN ROTOR MOSES-Calculations vs. Whirl Tower Results

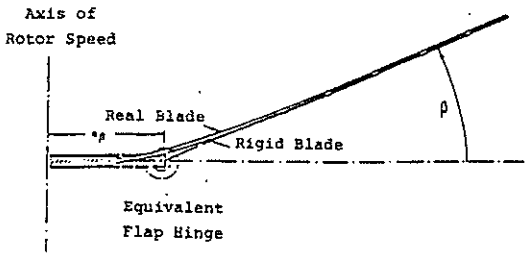

Fig. 2.1d: Principle of Equivalent Rigid Blade Body System

End forces and deflections for massless beam

Free-body diagram of mass m_i

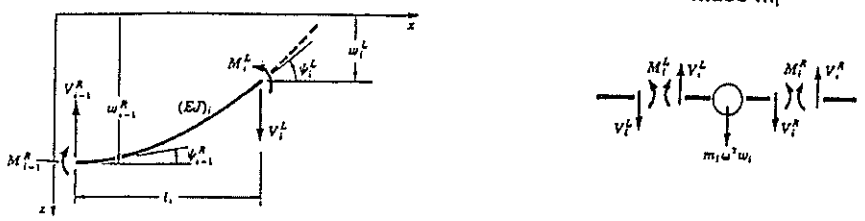

(shear force V, moment M, slope ψ, deflection w, flexural stiffness EJ, length l, mass m, rotation velocity ω)

Fig. 2.1b: Principle of Transfer Matrix Method example: Beam Bending without Centrifugal Force

Double Beam BO 105, TIGER

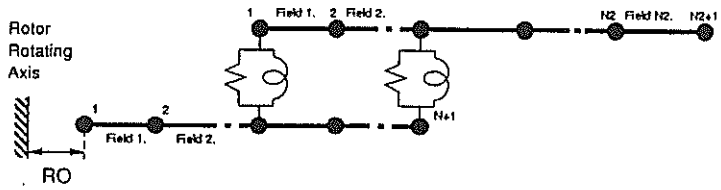

Fig. 2.1c: Modelisation of Blade and Hub in MOSES

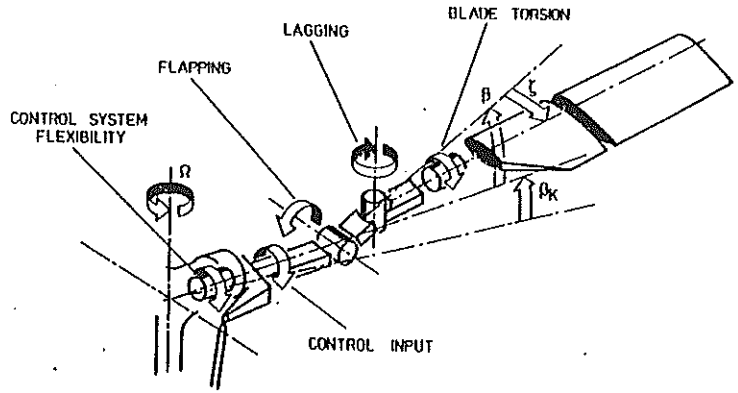

Fig. 2.2a: Analytical Model used in codes STAN, BWVL

Flap Bending vs. azimuth

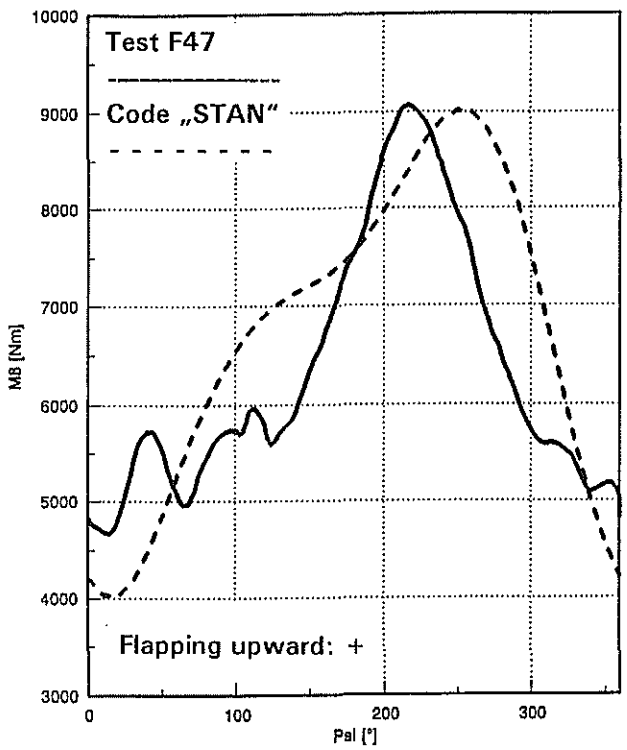

Lag Bending vs. azimuth

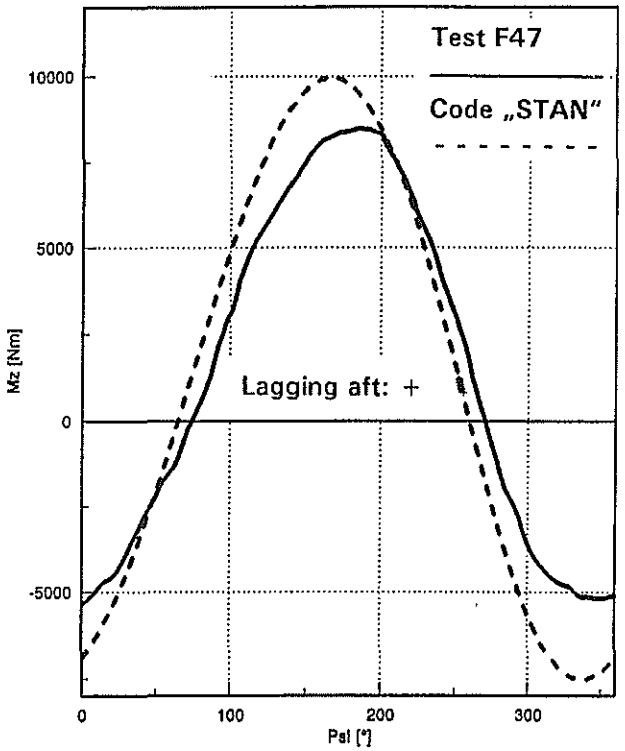

Rotating Pitch Link Load vs. azimuth

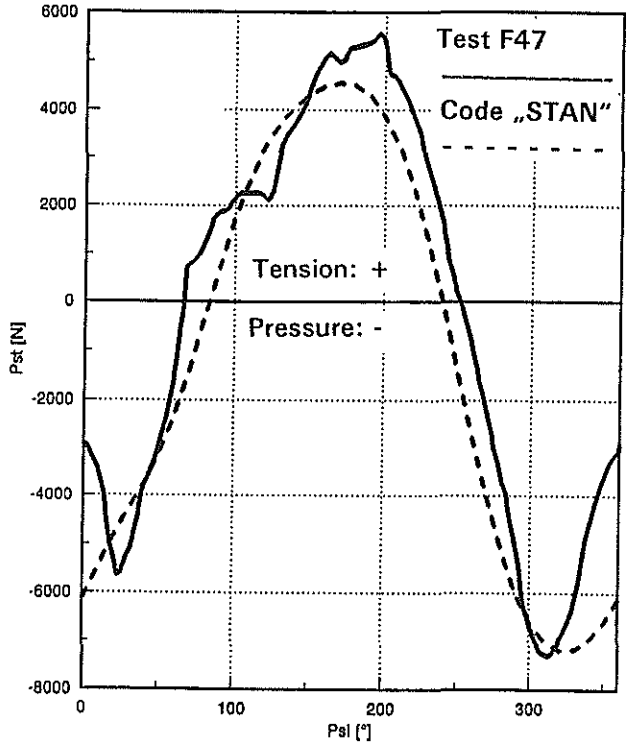

Comparison: Test results F47/Calculation with code „STAN"
Spiral Turn (coordinate curve with collective const.):
H = 3500 [ft]; G = 4806 [kg]; Vias = 100 [kts]; nz = 2.4 g; CT/σ = 0.16

Fig. 2.2b: Recalculation of first test results of the main rotor (DROOP version)

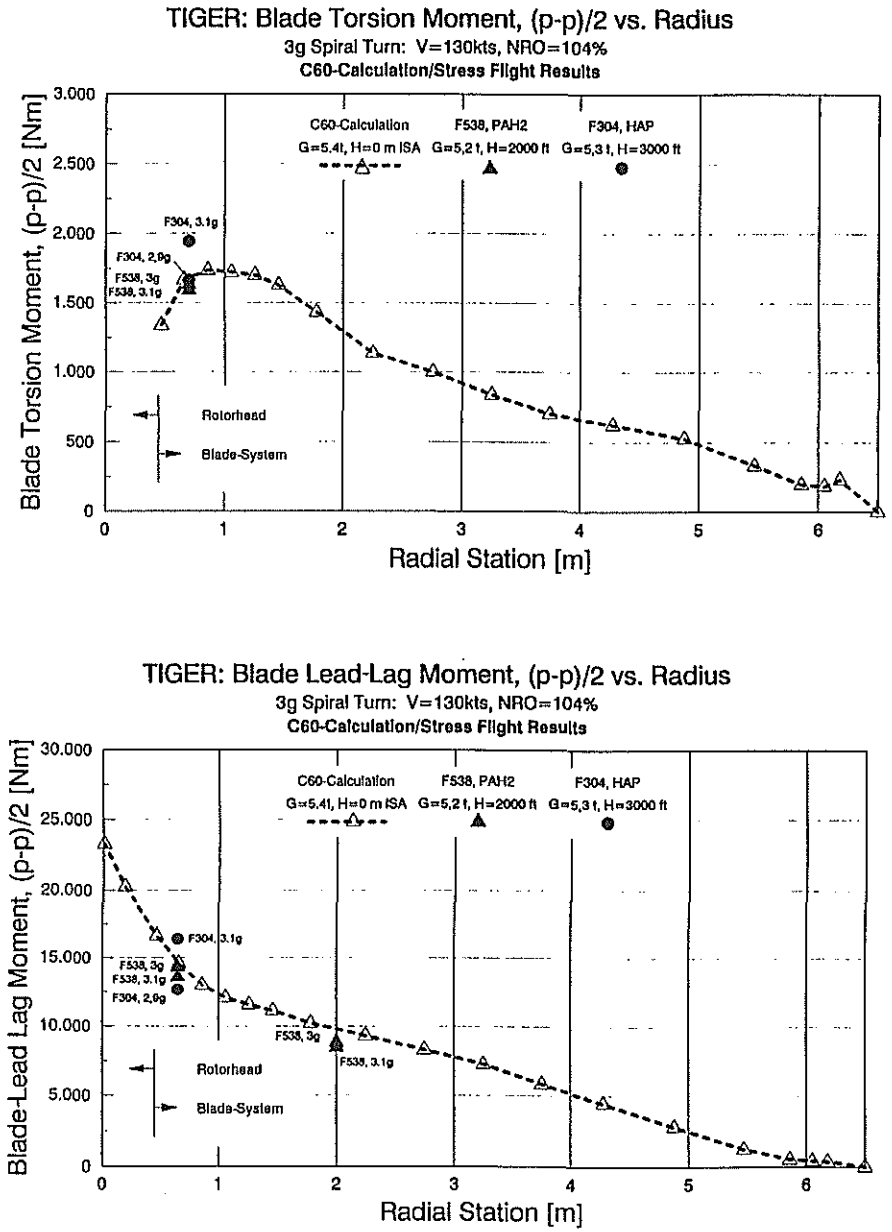

Fig. 2.3: TIGER: Blade Loads vs. Radius C60 Calculations/Flight Test Results

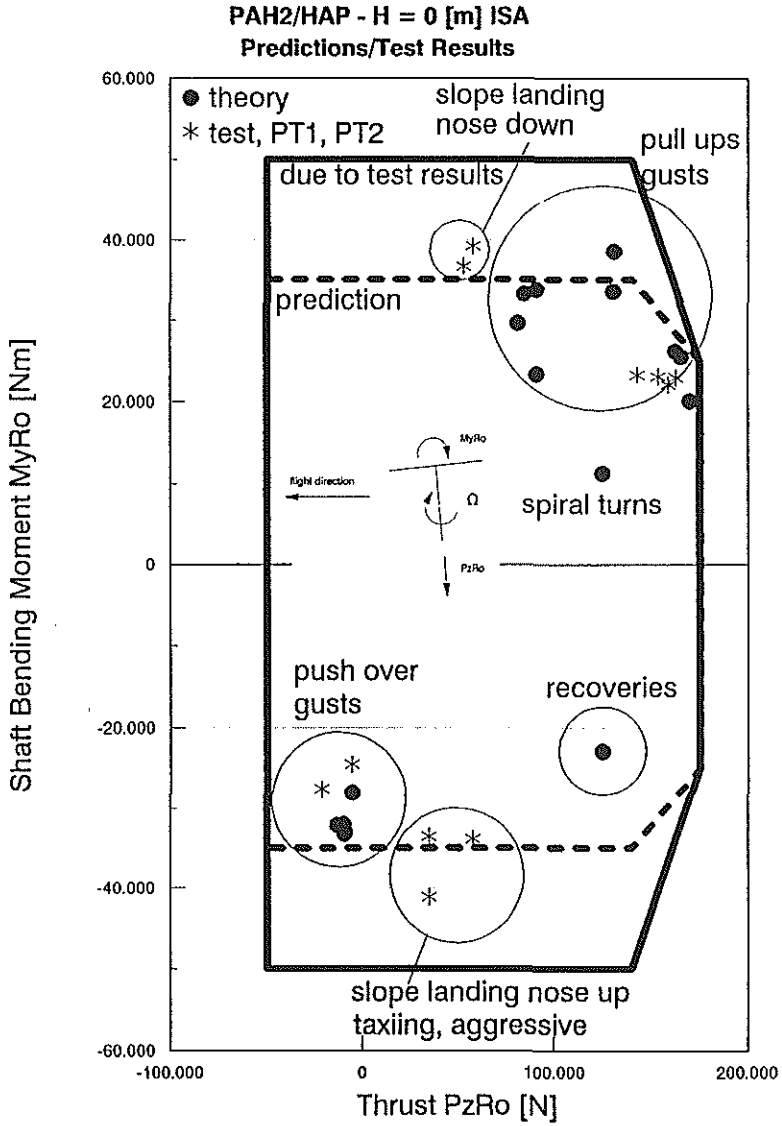

Fig. 2.4: TIGER: Thrust /Mast Moment-Envelope BWVL-predictions vs. fixing after flight tests

Anti-Vibration System „SARIB"

The „SARIB"-System filters 4/REV-vibrations from the main rotor in vertical, pitch and roll direction. Tuning is accomplisched by the flapper masses

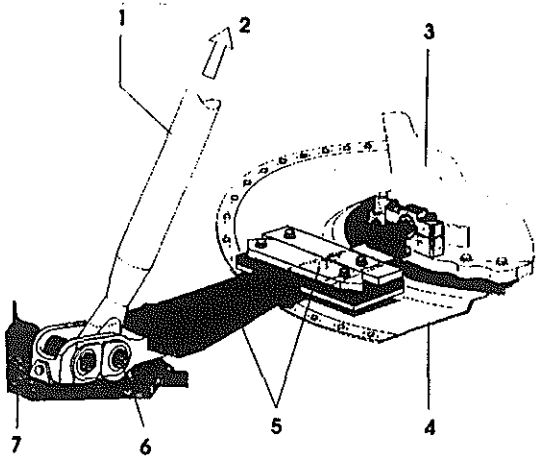

1 Suspension rod transmitting lift
2 To the rotor head
3 Floating main gear box
4 Flexible diaphragm transmitting torque
5 Flexible plate and vibrating mass
6 Leverage
7 Fitting anchored to the structure

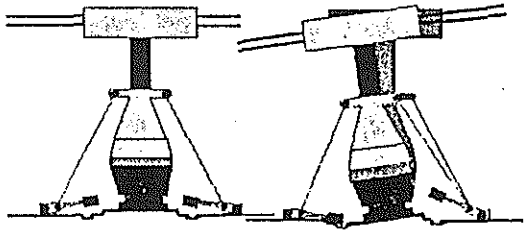

Fig. 3.2a: Anti-Vibration System „SARIB"

4/REV Cockpit Vibration vs. airspeed (test results)

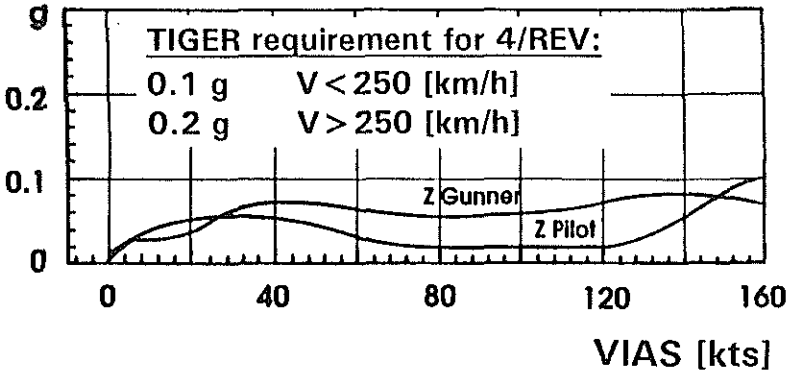

Fig. 3.2b: 4/REV cockpit vibrations vs. speed

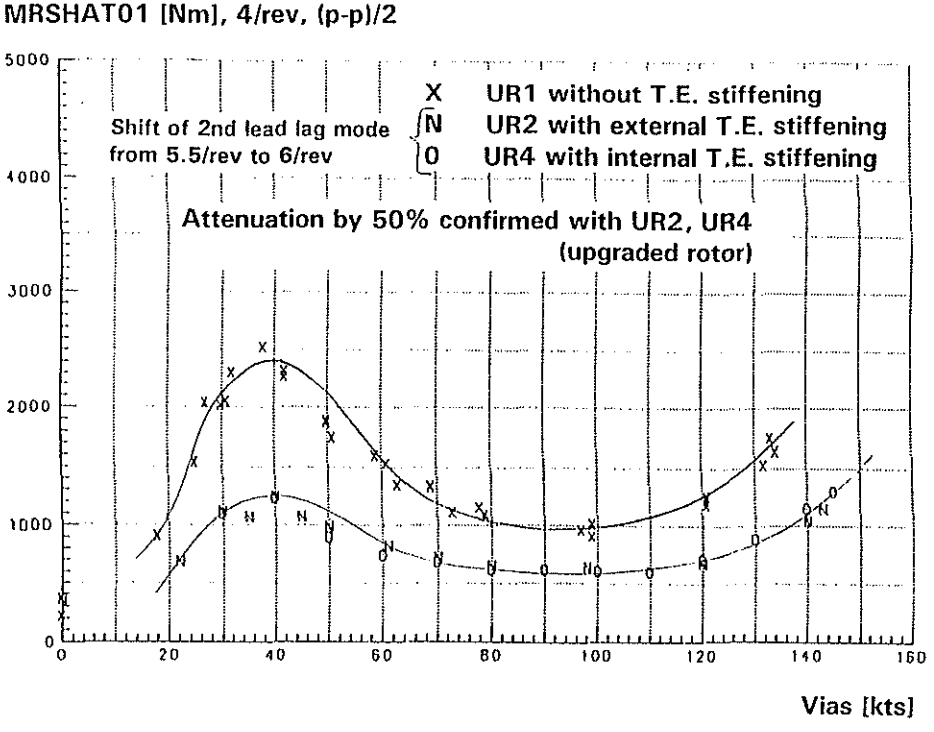

Fig. 3.3: Torque Modulation (4/REV) in Level Flight

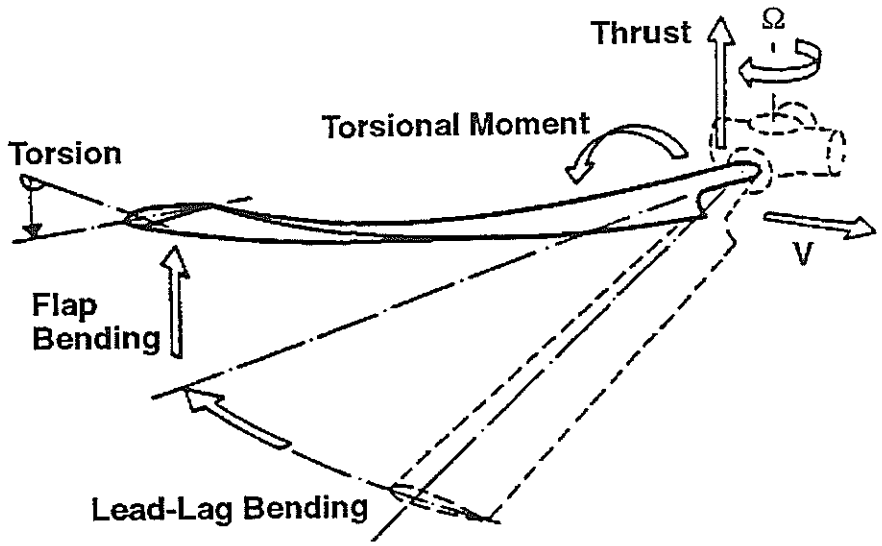

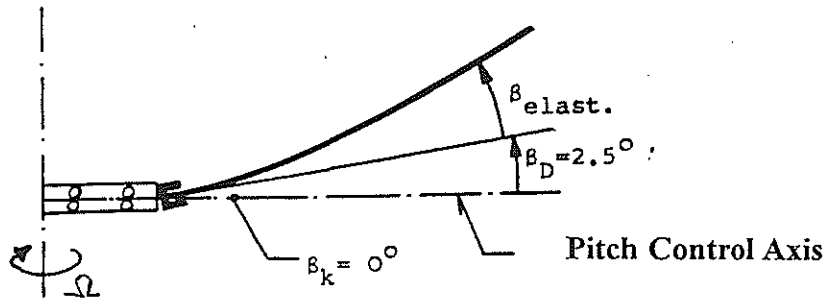

DROOP

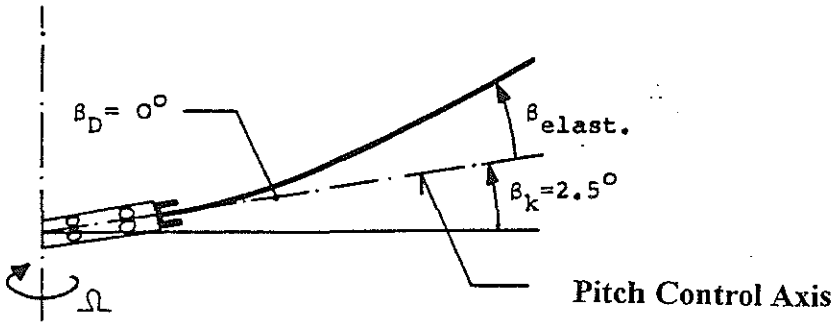

PRECONE

Note: (Flap - Lead-Lag Bending) can contribute significantly to the blade torsional moment. Due to its greater distance to the pitch control axis the DROOP rotor blade generates higher lead-lag bending and control loads refered to the same cyclic control input.

β_K Hub built-in PRECONE Angle
β_D Blade built-in DROOP Angle
$\beta_{elast.}$ Elastic Blade Flapping Angle

Fig. 3.4a: Kinematics of DROOP and PRECONE

C60 calculation
coordinate spiral turn: nz = 2.5g; H = 0 [m] ISA; NRO = 104 [%]; G = 5400 [kg]; V = 120 [kts]

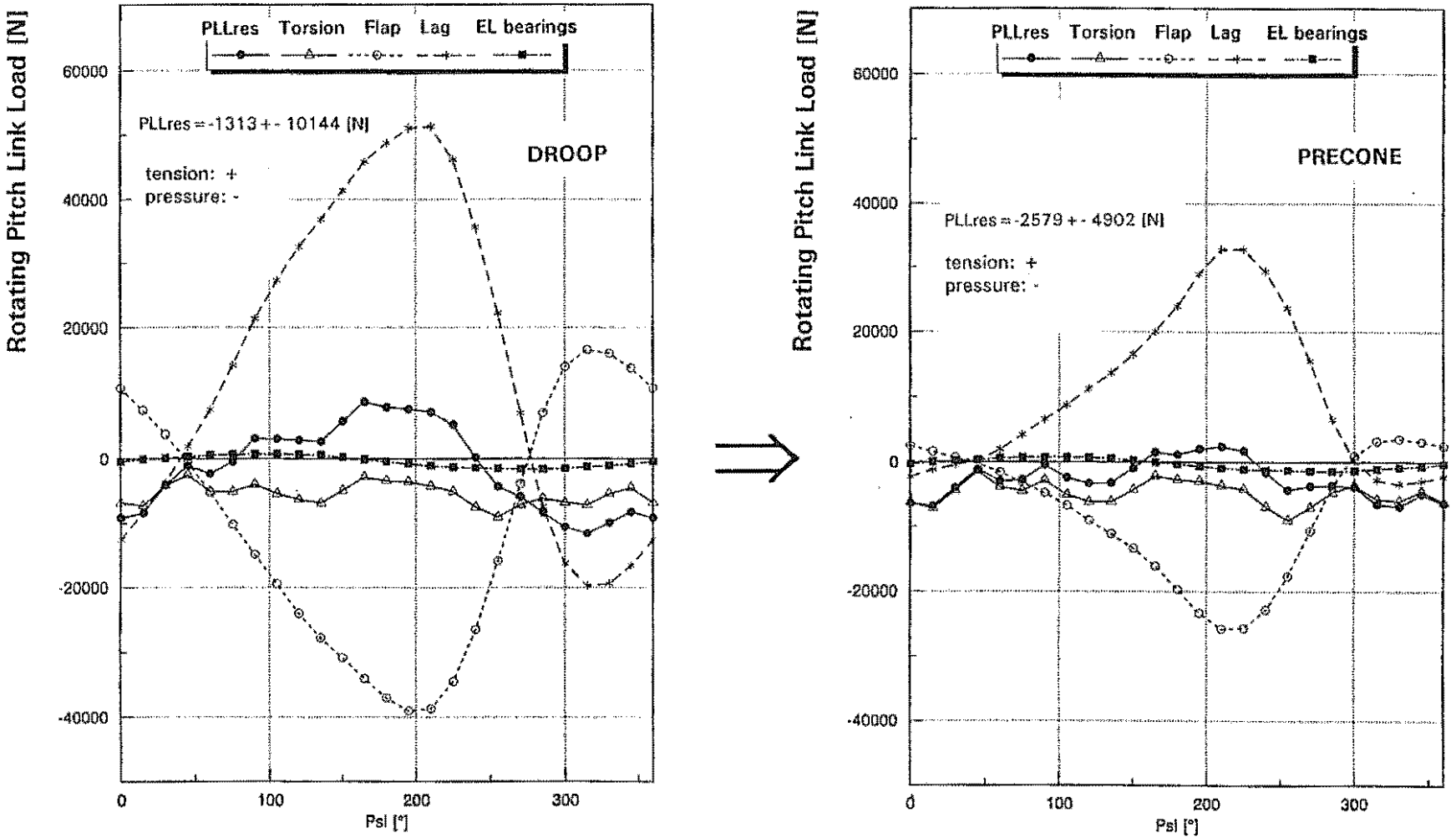

Fig. 3.4b: Reduction of rotating pitch link loads by attenuation of flap/lag torsional bending

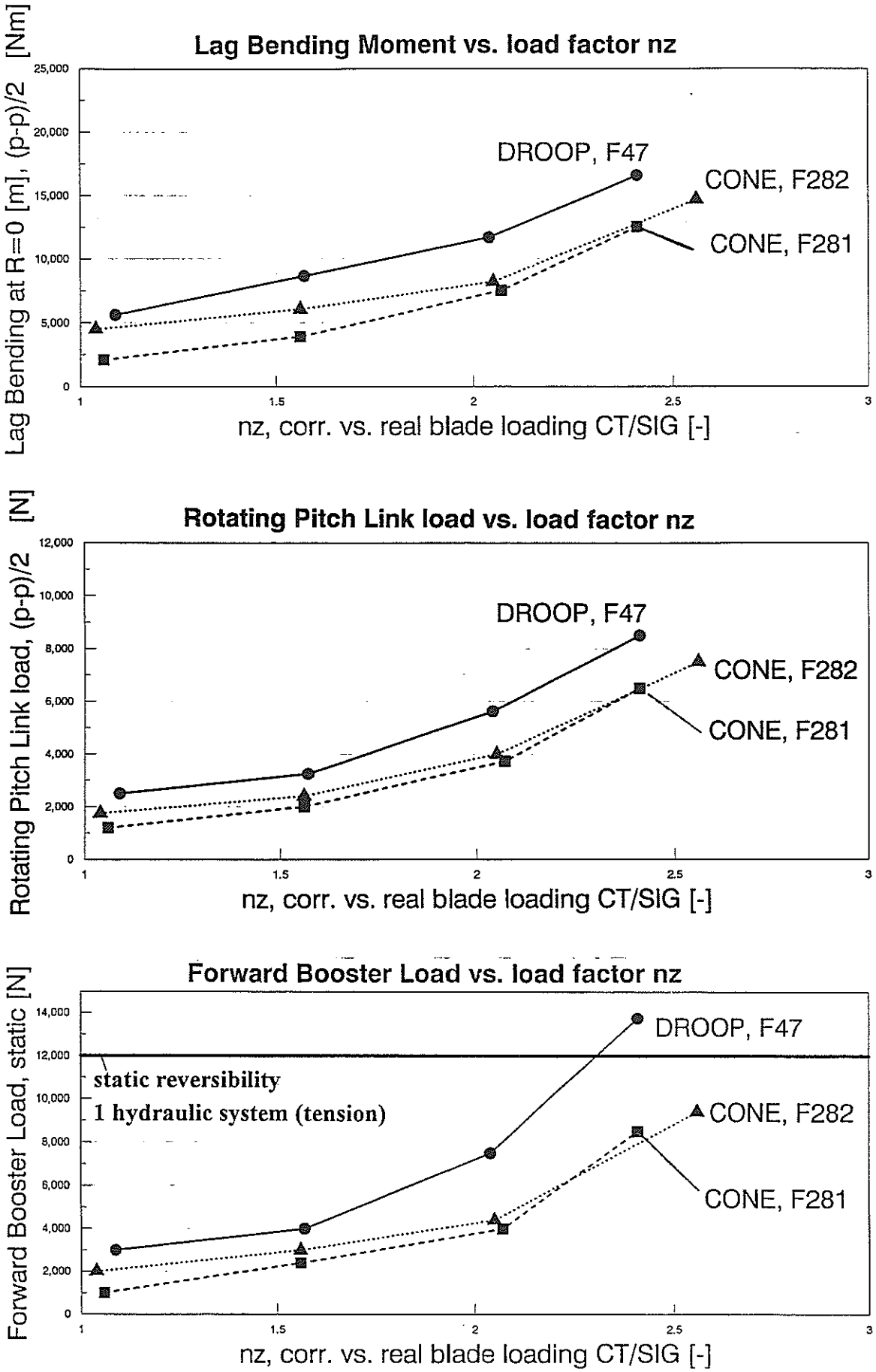

Fig. 3.4c: **Hub Geometry Change: DROOP → PRECONE**
Proof by Flight Test: Results from F47; F281, F282
coordinate spiral turns, V=120 [kts], H=2000 [ft]

Table 4: TIGER Flight Spectrum*)

	time [%]
Ground Run	4.30
Vertical Take off; normal Landing	0.80
Taxiing	2.90
HIGE	8.00
HOGE	15.00
Hovering with wind	0.10
Hover, control reversals	3.00
Level Flight 20% - 50% VNE	7.30
Level Flight 80% VNE, MCP	24.30
VNE, VDIVE	0.10
Sideward Flights, Rearward Flight	2.00
Climb, Partial Power Descent	8.50
Transitions (Power <--> AR; accel. flight ...etc.)	2.10
Pull ups, coll. & cyclic	0.80
Push overs	0.50
Flare, Quickstop	1.80
Spiral Turns at 50%, 80%, 100% VNE	8.20
Level Turns (constant height)	1.40
Rolling pull out	0.50
Spot Turns	1.00
S-Turns (lateral jinking)	1.50
Control reversals at 80% VNE	2.30
Landing Approach	0.90
Autorotation	1.80
Slope Landings	0.10
O.E.I Flights	0.80
	Σ 100.00

*) for convenience:
- simplified spectrum, rounded percentages
- variations in athmospheric conditions, gross weight, center of gravity, level of aggressivity (from moderate to very aggressive), sideslip, NRO not shown here

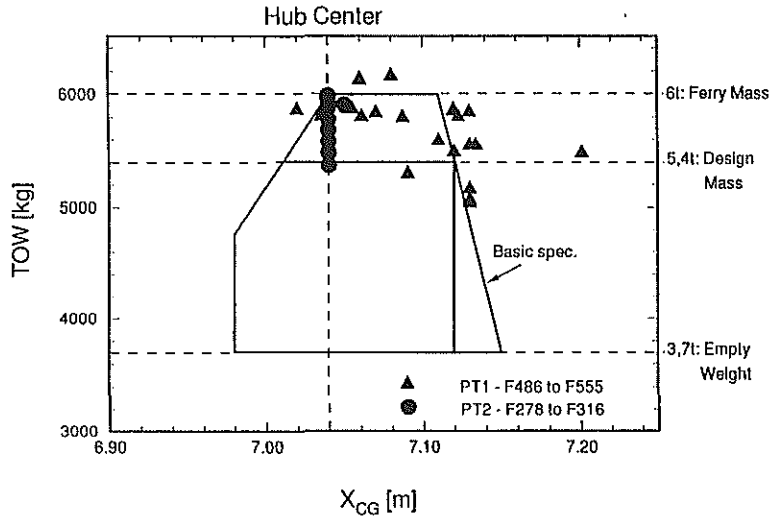

Fig. 4.1: Weight/C.G. - Combinations demonstrated during Stress Flight Campaign

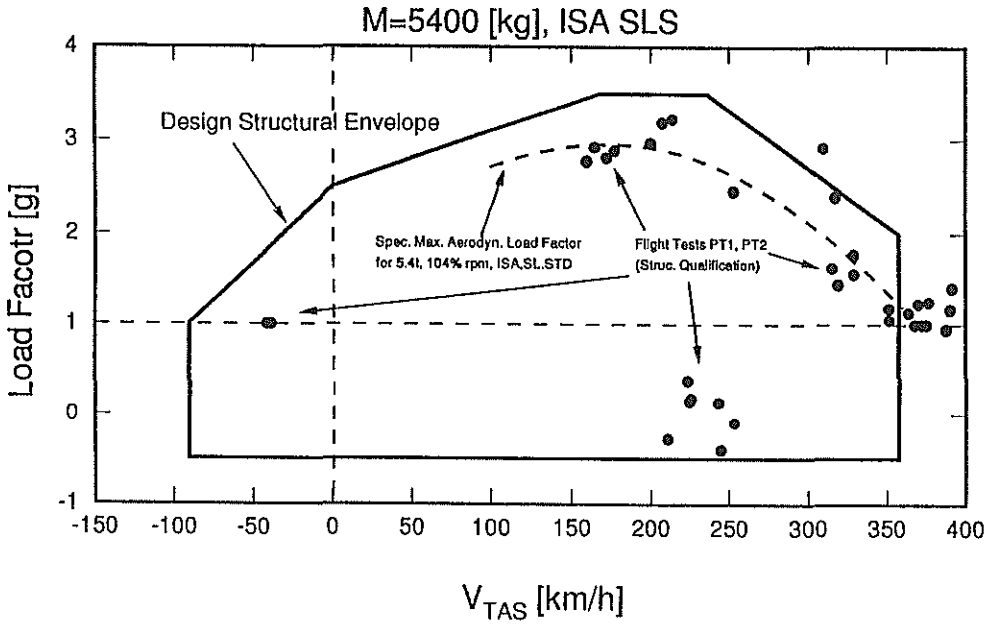

Fig. 4.2: Load Factor/Speed-Envelope (Structural Qualification)

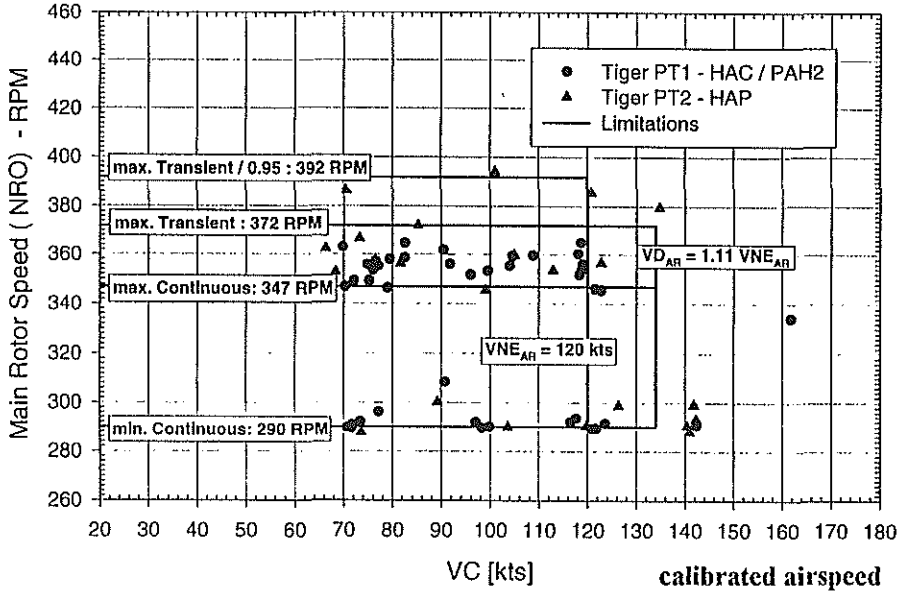

Fig. 4.3: Demonstrated Rotor Speed Range acc. to FAR §29

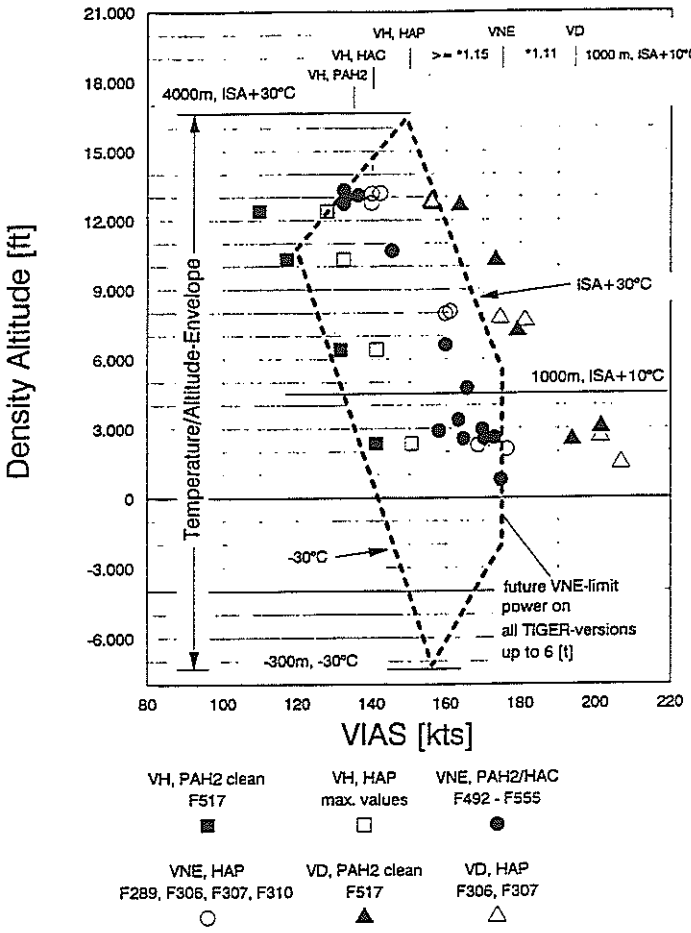

Fig. 4.4: Altitude/Temperature/Speed-Envelope (Stress Flight Results: PAH2/HAC, HAP)

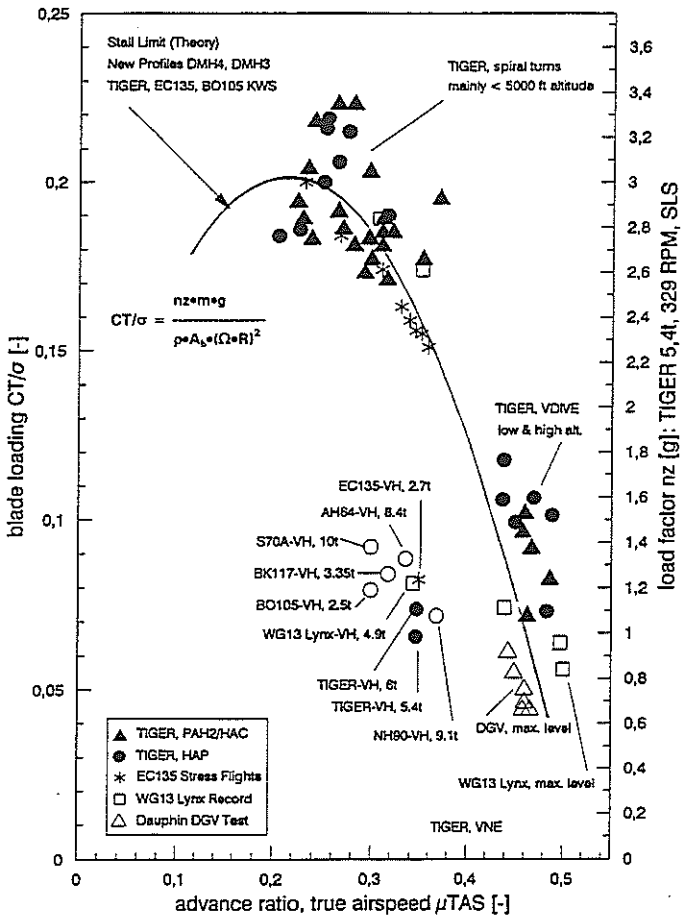

Fig. 4.5: Load Factor/Speed Capability (Stress Flight Results: PAH2/HAC, HAP) Comparison with other Helicopters

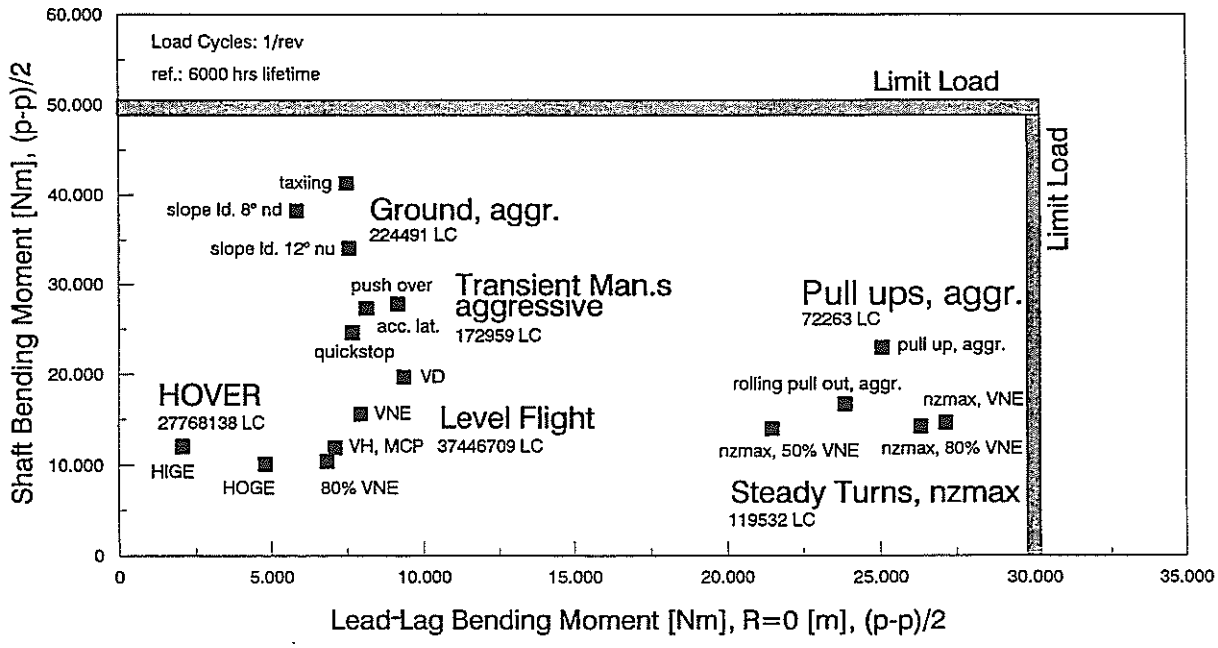

Fig. 4.6: Mast Bending Moment vs. Lead-Lag Bending Moment Design Limits and Stress Flight Results, TIGER PT1/2